Research Article | Vol. 25, No. 4 | 20 Feb 2017 | OPTICS EXPRESS 4509

Optics EXPRESS

Improved thickness estimation of liquid water using Kramers–Kronig relations for determination of precise optical parameters in terahertz transmission spectroscopy

HEYJIN SON,[1,2,3] DA-HYE CHOI,[1,2,3] AND GUN-SIK PARK[1,2,*]

[1]*Department of Physics and Astronomy, Seoul National University, Seoul 08826, South Korea*
[2]*Center for THz-driven Biomedical Systems, Seoul National University, Seoul 08826, South Korea*
[3]*These authors contributed equally to this work*
[*]*gunsik@snu.ac.kr*

Abstract: In terahertz transmission spectroscopy, there is a typical problem of thickness uncertainty, which hampers to determine precise optical parameters of samples. In order to resolve this experimental problem, a method optimizing sample thickness using singly subtractive Kramers–Kronig relations is proposed. For tens of micrometers thick water samples, we improved the accuracy of sample thickness by an order of magnitude (up to sub-micrometer) using the algorithm leading to obtain precise optical parameters of water. The broad applicability of the method is demonstrated for measuring various materials in addition to highly absorbing liquid water in the spectral range from 0.3 to 1.6 THz.

OCIS codes: (300.6495) Spectroscopy, terahertz; (000.3860) Mathematical methods in physics; (120.7000) Transmission.

References and links

1. M. Walther, B. Fischer, M. Schall, H. Helm, and P. U. Jepsen, "Far-infrared vibrational spectra of all-trans, 9-cis and 13-cis retinal measured by THz time-domain spectroscopy," Chem. Phys. Lett. **332**(3), 389–395 (2000).
2. D. M. Mittleman, R. H. Jacobsen, R. Neelamani, R. G. Baraniuk, and M. C. Nuss, "Gas sensing using terahertz time-domain spectroscopy," Appl. Phys. B **67**(3), 379–390 (1998).
3. J. T. Kindt and C. A. Schmuttenmaer, "Far-infrared dielectric properties of polar liquids probed by femtosecond terahertz pulse spectroscopy," J. Phys. Chem. **100**(24), 10373–10379 (1996).
4. Ch. Fattinger and D. Grischkowsky, "Point source terahertz optics," Appl. Phys. Lett. **53**(16), 1480–1482 (1988).
5. D. H. Auston, "Picosecond optoelectronic switching and gating in silicon," Appl. Phys. Lett. **26**(3), 101–103 (1975).
6. W. Withayachumnankul, B. M. Fischer, and D. Abbott, "Material thickness optimization for transmission-mode terahertz time-domain spectroscopy," Opt. Express **16**(10), 7382–7396 (2008).
7. L. Duvillaret, F. Garet, and J.-L. Coutaz, "Highly precise determination of optical constants and sample thickness in terahertz time-domain spectroscopy," Appl. Opt. **38**(2), 409–415 (1999).
8. T. D. Dorney, R. G. Baraniuk, and D. M. Mittleman, "Material parameter estimation with terahertz time-domain spectroscopy," J. Opt. Soc. Am. A **18**(7), 1562–1571 (2001).
9. I. Pupeza, R. Wilk, and M. Koch, "Highly accurate optical material parameter determination with THz time-domain spectroscopy," Opt. Express **15**(7), 4335–4350 (2007).
10. M. Scheller, C. Jansen, and M. Koch, "Analyzing sub-100-μm samples with transmission terahertz time domain spectroscopy," Opt. Commun. **282**(7), 1304–1306 (2009).
11. M. Krüger, S. Funkner, E. Bründermann, and M. Havenith, "Uncertainty and ambiguity in terahertz parameter extraction and data analysis," J. Infrared Millim. Terahertz Waves **32**(5), 699–715 (2011).
12. S. P. Mickan, R. Shvartsman, J. Munch, X. C. Zhang, and D. Abbott, "Low noise laser-based T-ray spectroscopy of liquids using double-modulated differential time-domain spectroscopy," J. Opt. B Quantum Semiclassical Opt. **6**(8), S786–S795 (2004).
13. R. D. L. Kronig, "On the theory of dispersion of x-rays," J. Opt. Soc. Am. **12**(6), 547–557 (1926).
14. V. Lucarini, Y. Ino, K.-E. Peiponen, and M. Kuwata-Gonokami, "Detection and correction of the misplacement error in terahertz spectroscopy by application of singly subtractive Kramers–Kronig relations," Phys. Rev. B **72**(12), 125107 (2005).
15. M. Bernier, F. Garet, J. L. Coutaz, H. Minamide, and A. Sato, "Accurate characterization of resonant samples in the terahertz regime through a technique combining time-domain spectroscopy and Kramers–Kronig analysis," IEEE Trans. Terahertz Sci. Technol. **6**(3), 442–450 (2016).

#283055 https://doi.org/10.1364/OE.25.004509
Journal © 2017 Received 16 Dec 2016; revised 5 Feb 2017; accepted 10 Feb 2017; published 17 Feb 2017

Optics EXPRESS

16. V. Lucarini, J. J. Saarinen, and K.-E. Peiponen, "Multiply subtractive Kramers–Krönig relations for arbitrary-order harmonic generation susceptibilities," Opt. Commun. **218**(4), 409–414 (2003).
17. D. Grischkowsky, S. Keiding, M. Van Exter, and C. Fattinger, "Far-infrared time-domain spectroscopy with terahertz beams of dielectrics and semiconductors," J. Opt. Soc. Am. B **7**(10), 2006–2015 (1990).
18. V. Lucarini, J. J. Saarinen, K.-E. Peiponen, and E. M. Vartiainen, *Kramers–Kronig relations in optical materials research* (Springer Science & Business Media, 2005).
19. W. Withayachumnankul, B. M. Fischer, H. Lin, and D. Abbott, "Uncertainty in terahertz time-domain spectroscopy measurement," J. Opt. Soc. Am. B **25**(6), 1059–1072 (2008).
20. F. Yang, L. Liu, M. Song, F. Han, L. Shen, P. Hu, and F. Zhang, "Uncertainty in terahertz time-domain spectroscopy measurement of liquids," J. Infrared Millim. Terahertz Waves **38**, 1–19 (2016).
21. S. Woutersen and H. J. Bakker, "Ultrafast vibrational and structural dynamics of the proton in liquid water," Phys. Rev. Lett. **96**(13), 138305 (2006).
22. B. Born, H. Weingärtner, E. Bründermann, and M. Havenith, "Solvation dynamics of model peptides probed by terahertz spectroscopy. Observation of the onset of collective network motions," J. Am. Chem. Soc. **131**(10), 3752–3755 (2009).
23. J. Xu, K. W. Plaxco, and S. J. Allen, "Absorption spectra of liquid water and aqueous buffers between 0.3 and 3.72 THz," J. Chem. Phys. **124**(3), 036101 (2006).
24. W. J. Ellison, "Permittivity of pure water, at standard atmospheric pressure, over the frequency range 0–25 THz and the temperature range 0–100 C," J. Phys. Chem. Ref. Data **36**(1), 1–18 (2007).
25. R. Piesiewicz, C. Jansen, S. Wietzke, D. Mittleman, M. Koch, and T. Kürner, "Properties of building and plastic materials in the THz range," Int. J. Infrared Millieter Waves **28**(5), 363–371 (2007).

1. Introduction

Terahertz time-domain spectroscopy (THz-TDS) has been widely applied to study optical properties of liquids, solids and gases in the terahertz region [1–3] since its development in the 1980s and 1990s [4, 5]. In transmission THz-TDS measurement, the complex optical parameters of samples are calculated from amplitude and phase change of THz time-domain pulses after propagating through samples. In the measurement, the sample thickness should be precisely determined for obtaining accurate optical parameters [6]. It has been shown that inaccuracy in the thickness results in erroneous value of optical constants for optically thick and thin samples as well as undesirable fringe patterns caused by multiple reflections for thin samples [7, 8].

In the studies for optically thick samples, echoes occurring in the time domain signals are used for accurate optical parameters while for thin samples, minimization of unwanted ripples is the key idea for optimal optical constants [7, 8]. The methods are applicable to samples with low absorption, relatively high refractive index and/or more than a few hundreds of micrometer-thick materials. A following study made it possible to investigate samples about 100 μm with low indexes of refraction [9] by introducing an iterative algorithm using spatially moving average filter (SVMAF) for finding the accurate material parameters within the confidence intervals. Another study investigated sub-100 μm samples [10] by applying Fourier transform to the material parameters showing periodic oscillations making a discrete peak which has to be minimized. The authors mentioned that the system's bandwidth is the limiting factor of the smallest determinable thickness [10].

For highly absorbing materials such as liquid water, transmitted THz intensity critically decreases at frequencies beyond 1.5 THz [11]. As the dynamic range critically decreases with thickness of water, typical sample thickness is about 100 μm or less. In these circumstances, thickness accuracy is critical for precise optical parameters [12]. There are some experimental approaches to this issue. Some determined accurate sample thickness of liquids using a piezoelectric translator [12]. Also, the liquid sample thickness can be measured from additional Fourier Transform Infrared (FTIR) spectroscopy measurement [11], whereas uncertainty remains in every assembly of liquid cells. Here, we propose an algorithm of rigorous optical parameter extraction for high absorbing material without any additional measurements by thickness optimization using Kramers–Kronig (K–K) relations.

K–K relations correlate between real and imaginary parts of the optical constants without prior assumptions [13]. Typically, THz-TDS is a spectroscopy that does not require K–K relations, unlike many of the other spectroscopic tools to obtain the real part of the complex

Optics EXPRESS

optical constant. In other words, this implies that we can obtain additional information about optical constants from K–K relations. In this context, researchers utilized K–K relations to detect and correct the misplacement error in the THz reflection [14] and to retrieve the lost phase information in the THz transmission spectroscopy [15]. In this paper, we propose an algorithm for accurate optical parameter of samples in the THz range, applicable even to high absorbing liquid water, using singly subtractive Kramers–Kronig (SSKK) relations as SSKK is applicable to finite bandwidth data and also provides rapid convergence of integral [16]. The broad applicability of the method is demonstrated for measuring various materials including highly absorbing liquid water in the spectral range from 0.3 to 1.6 THz.

2. Optical parameter extraction algorithm

The entire process of optical parameter extraction algorithm is depicted in Fig. 1. The algorithm is organized in two parts: error minimization by introducing theoretical transfer function and thickness optimization using K–K relations. In the subsequent section, we present each part in detail.

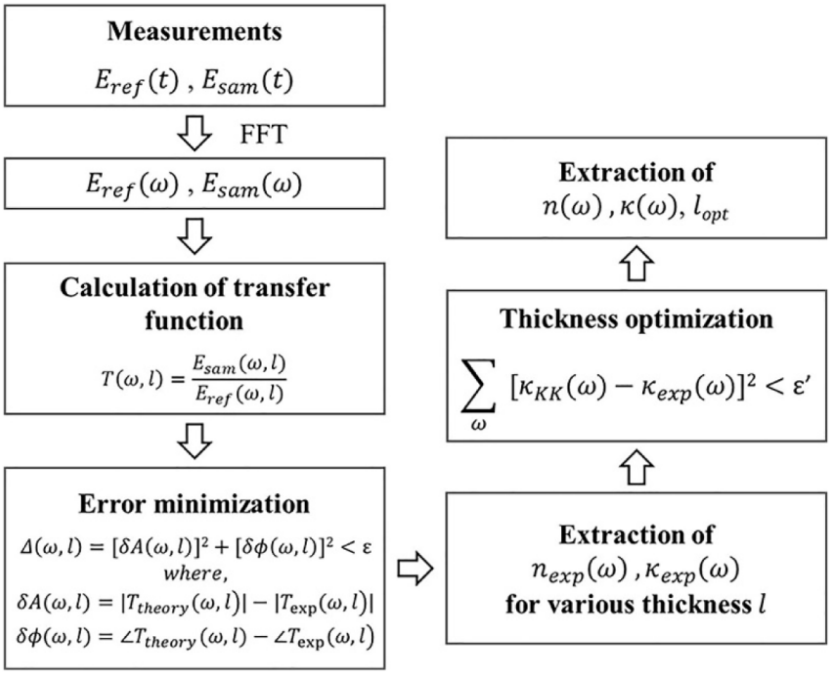

Fig. 1. Block diagram of the optimization procedure.

2.1 Error minimization by introducing theoretical transfer function

Here, we introduce an analytic formula of THz wave propagating a liquid sample. Figure 2 illustrates the experimental configuration of liquid sample measurement. The liquid is sandwiched between two polished THz windows and THz time-domain pulse profiles with and without liquid are measured. We choose z-cut quartz as a window material due to its low-loss and less-dispersion in the THz frequency range [17]. To avoid multiple reflections inside the window, 2 mm-thickness of quartz window is used.

When we introduce the transfer function, the sample is assumed to be homogeneous with parallel and planar surfaces. We also assume normal incidence of THz wave. Rationales of the assumptions are given elsewhere [8, 9].

Optics EXPRESS

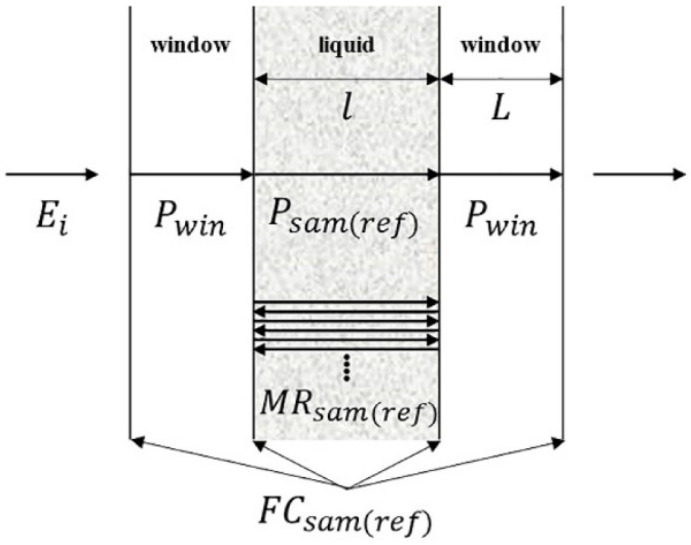

Fig. 2. Schematic diagram of transmitted THz wave through the liquid sample (not to scale).

The transfer function $T(\omega)$ is given by the ratio of reference $E_{ref}(\omega)$ and sample $E_{sam}(\omega)$ signals, which are Fourier transformed from time-domain pulses. The transfer function includes five elements: the initial electric field E_i, propagation inside window P_{win} and sample (reference) P_{sam} (P_{ref}), Fresnel coefficients at interfaces FC_{sam} (FC_{ref}) and multiple reflections inside sample (reference) MR_{sam} (MR_{ref}).

$$T(\omega) = E_{sam}(\omega) / E_{ref}(\omega) \tag{1}$$

$$E_{sam(ref)} = E_i \cdot P_{win}(\omega, L) \cdot P_{sam(ref)}(\omega, l) \cdot FC_{sam(ref)}(\omega) \cdot MR_{sam(ref)}(\omega, l),$$

where

$$P_{win}(\omega, L) = \exp(i\omega n^*_{win} L / c),$$

$$P_{sam(ref)}(\omega, l) = \exp(i\omega n^*_{sam(air)} l / c),$$

$$FC_{sam(ref)}(\omega) = \frac{2n^*_{air}}{n^*_{air} + n^*_{win}} \cdot \frac{2n^*_{win}}{n^*_{win} + n^*_{sam(air)}} \cdot \frac{2n^*_{sam(air)}}{n^*_{sam(air)} + n^*_{win}} \cdot \frac{2n^*_{win}}{n^*_{win} + n^*_{air}}, \tag{2}$$

$$MR_{sam(ref)}(\omega, l) = \sum\nolimits_{j=0}^{m_{sam(ref)}} \left[\left(\frac{n^*_{win} - n^*_{sam(air)}}{n^*_{win} + n^*_{sam(air)}} \right) \cdot \exp\left(i\omega n^*_{sam(air)} l / c \right) \right]^{2j}.$$

Here, n^*_{win} ($= n_{win} + i\kappa_{win}$), n^*_{sam} ($= n_{sam} + i\kappa_{sam}$) and n^*_{air} ($= n_{air} + i\kappa_{air}$) are complex refractive indices of window, liquid and air, respectively. c is the speed of light, and L and l denote window and sample (or air) thickness. $m_{sam(ref)}$, a maximum number of multiple reflections inside liquid (air), is calculated using the following inequality.

$$1 + 2m_{sam(ref)} \le \frac{c \cdot W}{n_{ini(air)} \cdot l}, \qquad \text{where } n_{ini} = n_{air} + \frac{c \cdot \Delta t}{l}. \tag{3}$$

Δt is the time difference of maximum amplitude of reference and sample time-domain signals. W is the length of measurement time window. Optical constants of the liquid for various sample thickness are obtained by minimizing error (Δ) between measured ($T_{exp}(\omega, l)$) and theoretical ($T_{theory}(\omega, l)$) transfer functions. Hereafter, optical constants calculated from error minimization are referred to as n^*_{exp} ($= n_{exp} + i\kappa_{exp}$).

Optics EXPRESS

$$T_{exp}(\omega,l) = \left|T_{exp}\right| \exp(i\angle T_{exp}),$$
$$T_{theory}(\omega,l) = \frac{FC_{sam}(\omega,l)\cdot P_{sam}(\omega,l)\cdot MR_{sam}(\omega,l)}{FC_{ref}(\omega,l)\cdot P_{ref}(\omega,l)\cdot MR_{ref}(\omega,l)}. \quad (4)$$

$$\Delta(\omega,l) = [\delta A(\omega,l)]^2 + [\delta\phi(\omega,l)]^2,$$
where
$$\delta A(\omega,l) = \left|T_{theory}(\omega,l)\right| - \left|T_{\exp}(\omega,l)\right| \quad (5)$$
$$\delta\phi(\omega,l) = \angle T_{theory}(\omega,l) - \angle T_{\exp}(\omega,l).$$

2.2 Thickness optimization using Kramers–Kronig relations

Essence of the thickness optimization process is minimizing discrepancy between measured optical constant and calculated one by the K–K relations. Traditional K–K relations connect real and imaginary parts of optical constant ($n^* = n + i\kappa$) as follows:

$$n(\omega) = n(\infty) + \frac{2}{\pi} P\int_0^\infty \frac{\omega'\kappa(\omega')}{\omega'^2-\omega^2} d\omega',$$
$$\kappa(\omega) = -\frac{2}{\pi}\omega P\int_0^\infty \frac{n(\omega')-n(\infty)}{\omega'^2-\omega^2} d\omega' \quad (6)$$

where P denotes the Cauchy principal value and $n(\infty)$ is the real part of optical constant at the high frequency limit.

As the K–K relations require knowledge of refractive index in the whole frequency range, the integrands are known to be sensitive to information in the immeasurable frequency region. To relax the limitation of finite bandwidth, we exploit SSKK relations formulated by the subtractions $n(\omega)- n(\omega_0)$ and $\kappa(\omega)- \kappa(\omega_0)$. The point ω_0 is called an anchor point, where complex optical constant is known. Modified K-K relations for discrete summation are shown as follows.

$$n_{KK}(\omega,l) = n_{\exp}(\omega_0,l_{ini}) + \frac{2}{\pi}(\omega^2-\omega_0^2)\sum_{\omega'}\frac{\omega'\kappa(\omega',l)\Delta\omega'}{\left(\omega'^2-\omega^2\right)\left(\omega'^2-\omega_0^2\right)}$$
$$\frac{\kappa_{KK}(\omega,l)}{\omega} = \frac{\kappa_{\exp}(\omega_0,l_{ini})}{\omega_0} - \frac{2}{\pi}(\omega^2-\omega_0^2)\sum_{\omega'}\frac{[n(\omega',l)-n(\infty)]\Delta\omega'}{\left(\omega'^2-\omega^2\right)\left(\omega'^2-\omega_0^2\right)} \quad (7)$$

where l_{ini} and $\Delta\omega'$ are initially measured thickness of sample (air) and spectral resolution respectively.

We set the value of $n(\infty)$ to be 1 and choose the anchor point ω_0 where deviation of optical constants with thickness variation is minimal.

Although SSKK relations have been successfully applied to the finite bandwidth [ω_{min}, ω_{max}], the relations still have errors $e(\omega)$ due to frequency truncation [18]. We verified that the truncation errors from SSKK relations do not affect the value of optimized thickness.

$$e(\omega) = -\frac{2}{\pi}\omega\left(\omega^2-\omega_0^2\right)\left[\sum_{\omega'=0}^{\omega_{\min}}\frac{[n(\omega')-n(\infty)]\Delta\omega'}{\left(\omega'^2-\omega^2\right)\left(\omega'^2-\omega_0^2\right)} + \sum_{\omega'=\omega_{\max}}^{\infty}\frac{[n(\omega')-n(\infty)]\Delta\omega'}{\left(\omega'^2-\omega^2\right)\left(\omega'^2-\omega_0^2\right)}\right] \quad (8)$$

It has been shown that thickness uncertainty is the biggest error source to material refractive index both of solids [19] and liquids [20]. However, thickness uncertainty does not make the biggest contribution to uncertainty in absorption. We also confirmed that absorption is more insensitive to thickness variation than the refractive index, which will be shown in the

Optics EXPRESS

following section. Therefore, we defined total difference $Diff_{KK}$ between measured and calculated optical constants as below.

$$Diff_{KK}(l) = \sum_{\omega} [\kappa_{KK}(\omega, l) - \kappa_{\exp}(\omega, l)]^2 \quad (9)$$

Minimization of total difference $Diff_{KK}$ is conducted over 0.3-1.6 THz, and as a result, we determine both real and imaginary optical constants as well as optimized liquid thickness l_{opt} simultaneously.

3. Experimental results

In this section we give some experimental results that validate the algorithm proposed in the previous section. Optical constants of samples were obtained using a THz-TDS system (TAS7500SP, ADVANTEST Co.) with a transmission module. In the THz-TDS experiment, temporal form of THz wave is recorded with and without a sample. The temporal THz waveform with the sample experiences both amplitude decrease and time delay in comparison to the waveform without the sample. After Fourier transformation of the THz waveform, we can simultaneously obtain both the transmittance $T(\omega)$ and phase shift $\phi(\omega)$. Complex optical constant of the sample is calculated using the algorithm explained in the previous section.

3.1 Liquid water

The liquid samples were placed in a liquid cell with Teflon and aluminum spacers having various thickness (quoted thicknesses are 25, 56 and 100 μm for Teflon spacers and 50 μm for aluminum spacer) inserted between two z-cut quartz windows. All experiments were performed at room temperature. Typically, Teflon spacers are used for liquid cells [21, 22]. However, Teflon spacers are easy to compress such that mechanical measurement with an electronic micrometer does not provide the precise thickness. Therefore, researchers utilize FTIR measurements for determining the spacer thickness when it is assembled in the liquid cell as previously mentioned [11]. Still, spacer thickness measured by FTIR is not exactly the same with the thickness in a reassembled liquid cell used for the THz-TDS measurement. In order to compare the thickness obtained from the proposed algorithm and the measured thickness, we need a spacer that has low compressibility. In this sense, we first measured the optical parameter of liquid water with an aluminum spacer. Thickness of the spacer was measured with an electronic digital micrometer (Mitutoyo, No. 293-821) with 1 μm sensitivity and accuracy of ± 2 μm. The thickness measured with the micrometer screw is 49 μm for repeated 10 measurements.

Figure 3(a) THz field amplitude as a function of time after the transmission of the THz pulses through an empty liquid cell (reference) and through a cell filled with water (sample). Figure 3(b) depicts refractive index difference between measured value and calculated value over the sample thickness. The minimum of this curve is located at 49.1 μm, which is in excellent agreement with the measured thickness. We also estimate variation of the optimized thickness and confirm that the optimal thickness does not change with errors from finite bandwidth summation in SSKK relations. The insert graph shows a SSKK-calculated and a measured absorption coefficients at the optimized thickness. Discrepancy between measured and SSKK-calculated absorption coefficients originates from the value of n(∞), however, the optimized thickness does not change with the value of n(∞). These results demonstrate the validity of our algorithm for obtaining optimized thickness. Figures 3(c) and 3(d) represent the refractive index and absorption coefficient (= 2ωκ/c) of water obtained with the optimized thickness. The values match very well with the values obtained from the literature [23, 24]. We calculate influences of inaccurate sample thickness on optical constant to be 1.48 ± 0.06% per 1 μm for the real refractive index and 1.43 ± 0.48% per 1 μm for the absorption coefficient, while average experimental errors of repeat measurements are 0.14 ± 0.02% for the real refractive index and 0.37 ± 0.11% for the absorption coefficient. As

Optics EXPRESS

uncertainties from imprecise sample thickness exceed those from experimental errors, accuracy of the sample thickness should be improved approximately by an order of magnitude.

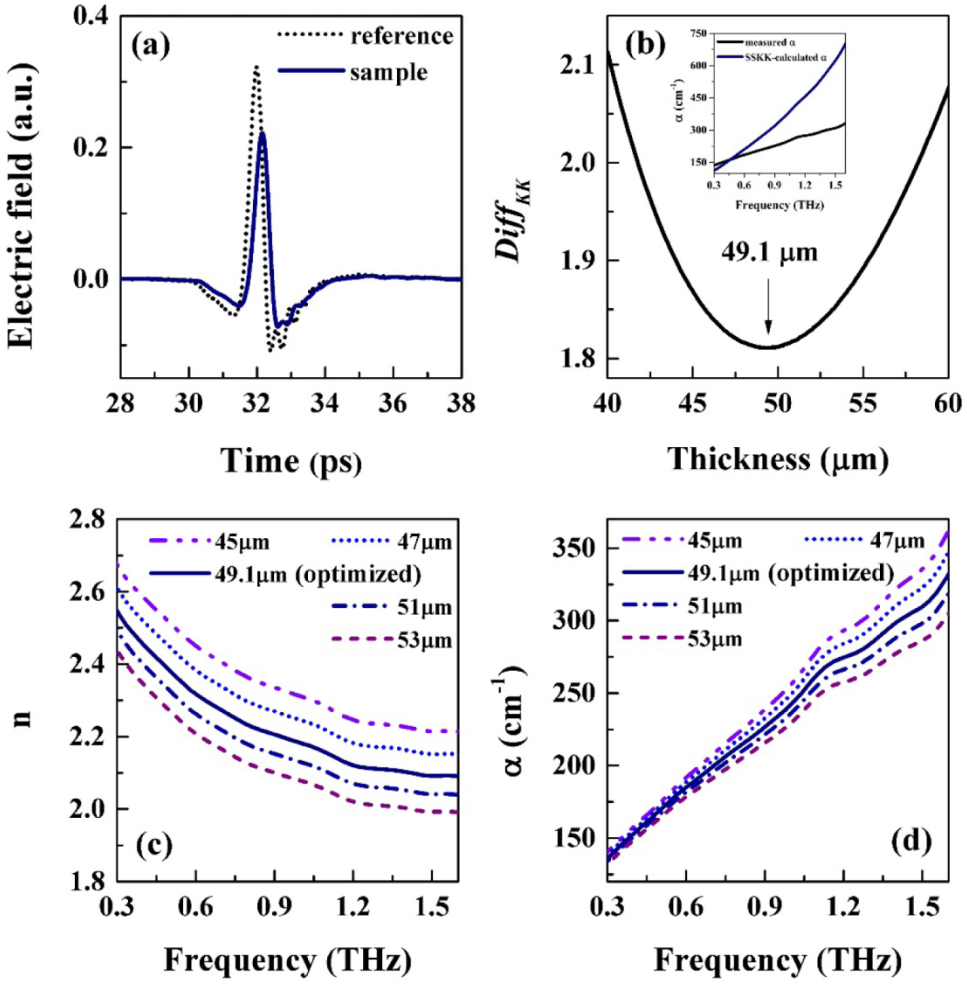

Fig. 3. Material parameter extraction of liquid water with a 50 μm-thick aluminum spacer (errors are within the linewidth)

To decide the anchor point, sensitivities of refractive index and absorption coefficient to thickness variation are examined. As shown in Fig. 4, absorption coefficient is less sensitive to thickness changing, and the anchor point has been chosen the minimum absorption coefficient variation for each measurement. For liquid water with a 50 μm-thick aluminum spacer, the average anchor point is 0.46 THz.

Optics EXPRESS

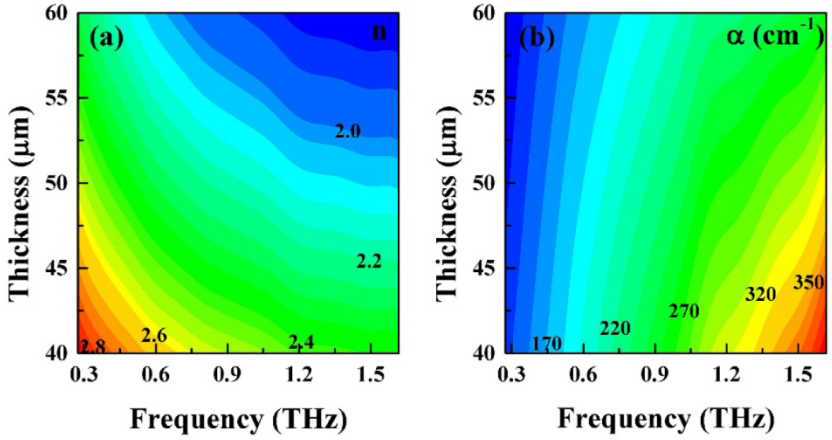

Fig. 4. Sample thickness and frequency dependence of (a) refractive index and (b) absorption coefficient of liquid water with a 50 μm-thick aluminum spacer

In the following, we obtain optical parameter of liquid water with Teflon spacers for practical use. Figures 5(a)-5(c) show refractive index difference between measured value and calculated value over the sample thickness for 25, 56 and 100 μm-thick Teflon spacers. Optimized thicknesses obtained from the algorithm are 26.2, 55.2 and 95.5 μm, respectively. Average anchor points of each thickness are 0.59 THz, 0.37 THz and 0.39 THz, respectively. Unlike the aluminum spacer, the Teflon spacer thickness is different from the quoted thickness as expected due to the compression in the liquid cell.

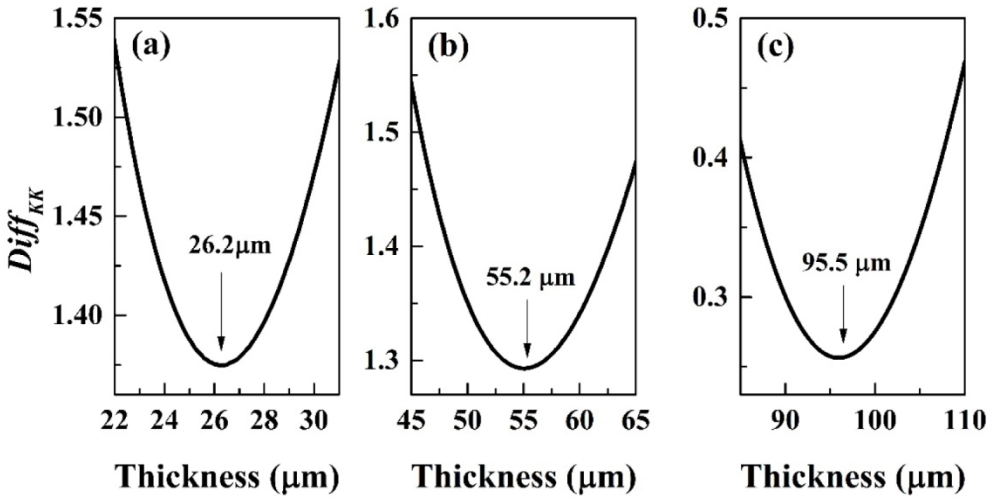

Fig. 5. Optimized thickness of (a) 25, (b) 56 and (c) 100 μm Teflon spacers.

Before we optimize the spacer thickness, optical parameters of liquid water obtained with different spacers are different as indicated in Figs. 6(a) and 6(b). Spectral curves Figs. 6(a) and 6(b) are obtained after Fabry-Perot removal. After the thickness is optimized, optical parameter of liquid water converges as shown in Figs. 6(c) and 6(d).

Optics EXPRESS

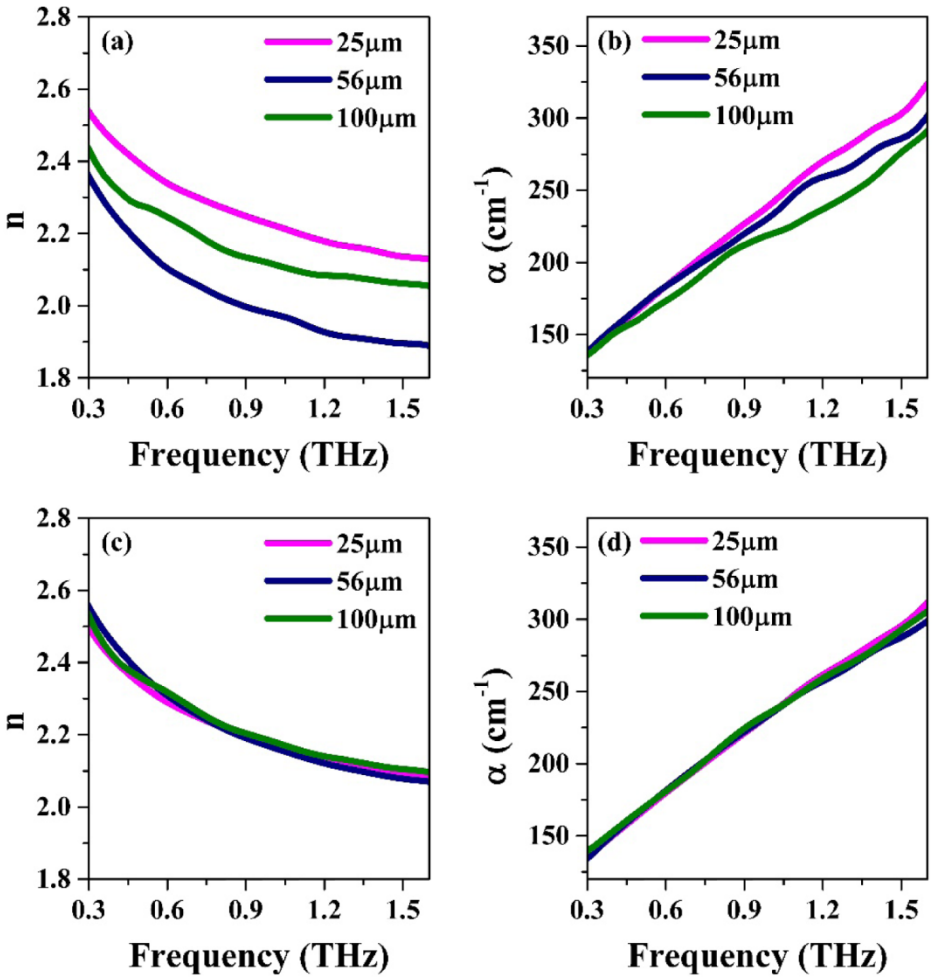

Fig. 6. Optical parameters of liquid water measured with Teflon spacers before ((a), (b)) and after ((c), (d)) thickness optimization.

3.2 Z-cut quartz and high-density polyethylene windows

As the algorithm does not have *a priori* assumptions about material properties it should be applicable to other materials. We obtain optical constants of mm-thick solids to demonstrate the broad applicability of the algorithm. Specifically, two different THz windows (1.e., z-cut quartz and high-density polyethylene (HDPE)) are chosen because accurate complex optical constant of the window is a prerequisite for determining precise optical constant of liquid samples. The measured thicknesses of a z-cut quartz window and a HDPE window are 2.070 and 2.979 mm, respectively. No multiple reflections are included in the time-domain signal for these window thicknesses. The optimized thickness of the quartz window is 2.066 mm as shown in Fig. 7(a), which is a perfect match with the measured value within the measurement error. The obtained optical constants presented in Figs. 7(b) and 7(c) are consistent with the literature value [17]. For example, at 1 THz, the measure index and absorption are 2.11 and 0.11 cm^{-1}, while the literature values are 2.11 and 0.14 cm^{-1}, respectively.

Optics EXPRESS

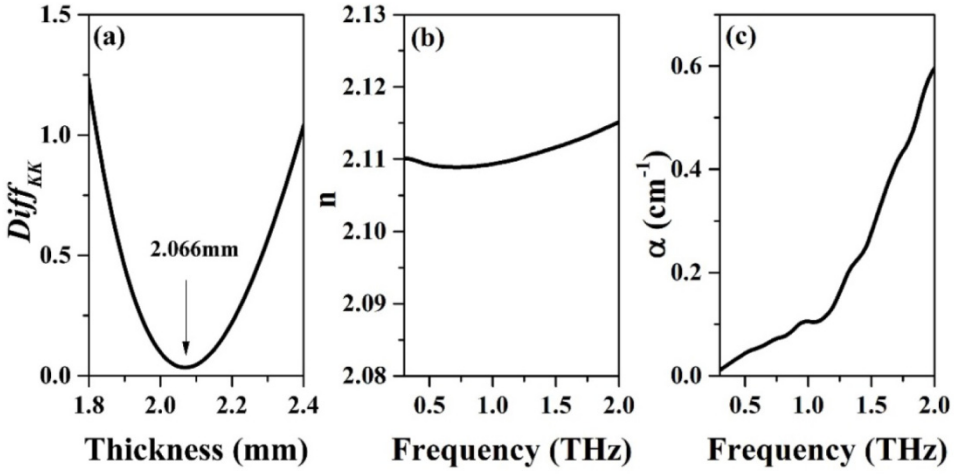

Fig. 7. Optimized thickness (a) and optical parameters ((b), (c)) of a z-cut quartz window.

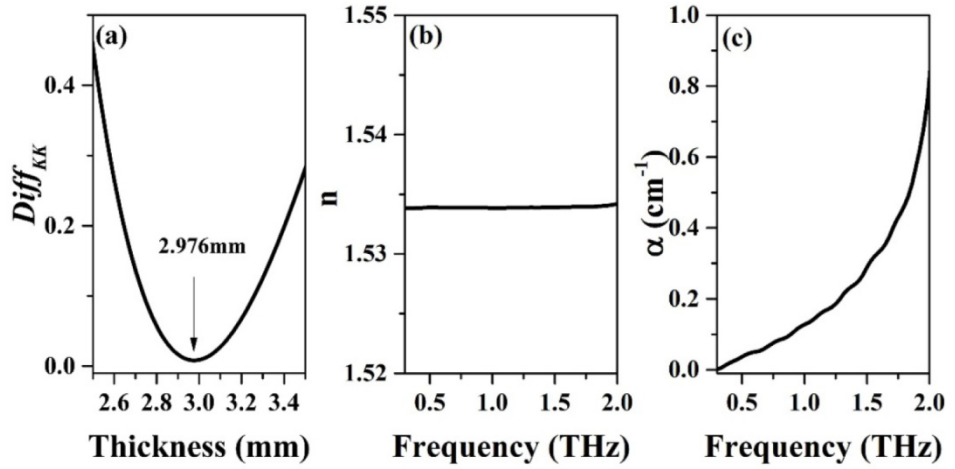

Fig. 8. Optimized thickness (a) and optical parameters ((b), (c)) of a HDPE window.

For the HDPE window, the optimized thickness is 2.976 mm as shown in Fig. 8. (a), which also shows good agreement with the measured value. The obtained optical constants are consistent with the literature value [25].

4. Conclusion

We propose an algorithm of rigorous optical parameter extraction for high absorbing material without any additional measurements by thickness optimization using SSKK relations. With this algorithm, we can simultaneously determine sample thickness and optical parameters of the highly absorbing liquid water in the spectral range from 0.3 to 1.6 THz. As the K–K relations are universal relations without any prior assumptions, this algorithm is not restricted to a particular system but suitable for many other experimental schemes.

Funding

National Research Foundation (NRF) Korean Government (MSIP) (2016R1A3B1908336).